Journal of Hazardous Materials 186 (2011) 1147–1153

Contents lists available at ScienceDirect

Journal of Hazardous Materials

journal homepage: www.elsevier.com/locate/jhazmat

Parametric studies of diethyl phosphoramidate photocatalytic decomposition over TiO_2

Bo Sun [a], Alexander V. Vorontsov [b,*], Panagiotis G. Smirniotis [a,**]

[a] Department of Chemical Engineering and Material Science, University of Cincinnati, Cincinnati, OH 45221-0012, USA
[b] Boreskov Institute of Catalysis, Novosibirsk 630090, Russia

ARTICLE INFO

Article history:
Received 29 June 2010
Received in revised form
13 November 2010
Accepted 27 November 2010
Available online 8 December 2010

Keywords:
Chemical warfare agent simulant
CWA
Tabun
Temperature
Aqueous suspension
Decontamination

ABSTRACT

The present study is focused on influences of parameters including pH, temperature, TiO_2 catalyst concentration, and reactant concentration on the rate of photocatalytic diethyl phosphoramidate (DEPA) decomposition with Hombikat UV 100 (HK) and Degussa P25 (P25) TiO_2. Total mineralization of DEPA is observed. Two regimes of pH, namely in acid and near-neutral environments were found where maximum total carbon (TC) decomposition was observed. The electrostatic effects on adsorption over the TiO_2 surface explain the above phenomena. The maximum rate is observed for P25 at DEPA concentration 1.3 mM whereas the rate grows continuously with DEPA concentration rise for HK. The temperature dependence of TC decomposition rate in the range of 15–63 °C with both HK and P25 follows the Arrhenius equation. The activation energy for total carbon decomposition with HK and P25 are 29.5 ± 1.0 and 24.3 ± 3.1 kJ/mol, respectively. The decomposition rate of DEPA is larger over P25 than over HK. The rate over P25 increases faster than that with HK for each unit of the titania added when the TiO_2 concentration is less than 375 mg/l. The higher light absorption and particles aggregation of P25 are responsible for the decrease of reaction rate we observed at catalyst concentration above a certain level. In contrast, the rate over HK increases monotonically with the concentration of the photocatalyst used.

1. Introduction

Decontamination of the hazardous chemical warfare agents (CWA) is required on the battlefield as well as in labs, pilot plants, and chemical agent production, storage, and destruction sites. [1] These agents are becoming a major threat to the environment and public safety. The safe destruction of these agents on a large scale is an important task [1,2]. Earlier works [1–17] indicated that semiconductor photocatalysis can mineralize some organic chemicals and CWA simulants completely and it is a promising solution for total destruction of CWA. The reaction can be carried out in atmospheric conditions. Among all the semiconductors used for photocatalysis, TiO_2 has proved to be the most feasible photocatalyst for its high photoactivity, inexpensiveness, chemical inertness and safety [2].

Previously, it was demonstrated that TiO_2 can decompose CWA simulants completely into inorganic products [15,18,19]. In this study, we will investigate photocatalytic decomposition of DEPA, a chemical simulant of Tabun (GA), with two mostly-used commercial TiO_2 Degussa P25 (P25) and Hombikat UV 100 (HK). The chemical structures of DEPA and GA both have the P–N bond connecting phosphorus and amine. Thus, it is important to test the operational conditions influence on destruction of this bond and the molecule as a whole.

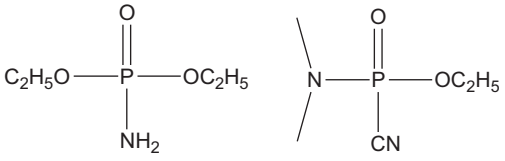

DEPA GA

In this investigation, the pH, the temperature, the catalyst concentration, and the DEPA concentration are considered as the key parameters. The optimal operation conditions for photocatalytic DEPA decomposition are found and the mechanistic implications are discussed. A double peak pH dependence of the mineralization rate was found for the first time.

2. Experimental

The catalysts utilized in the present study were commercial titania powders, Degussa P25 (P25) and Hombikat UV-100 (HK, Sachtleben Chemie GmbH). All reagents were used as received

* Corresponding author. Tel.: +7 383 326 9447; fax: +7 383 333 1617.
** Corresponding author. Tel.: +1 513 556 1474; fax: +1 513 556 3473.
E-mail addresses: voronts@catalysis.ru (A.V. Vorontsov), Panagiotis.Smirniotis@uc.edu (P.G. Smirniotis).

0304-3894/$ – see front matter © 2010 Elsevier B.V. All rights reserved.
doi:10.1016/j.jhazmat.2010.11.114

unless noted otherwise. The characteristics of these materials are readily available in the literature (e.g. [20,21]).

The suspension for reaction was prepared as follows. A predetermined amount of catalyst, a certain amount of DEPA (Aldrich), and 800 ml of distilled water (Nanopore, Steward) were mixed in a conical flask. The mixture was stirred for 10 min. The initial pH was adjusted further to study the effect of the pH with 0.5 M H_2SO_4 or 0.5 M NaOH solution. The resulting suspension was treated in an ultrasonic bath (Elma, Ultrasonic LC20H) for half an hour, heated to the desired temperatures and stirred for another 15 min afterwards. Measurements showed that DEPA was not removed from suspension during this procedure.

The photocatalytic oxidation of DEPA in the catalyst suspensions was carried out in an annular quartz liquid phase photocatalytic reactor (Ace glass, Inc., No.7840) previously described in [20]. The immersion-type UV radiation source was a 200 W medium pressure mercury vapor quartz lamp (Jelight, J05PM1HGC1). A Pyrex filter (Ace glass, No.7740) removed the far- and mid-UV bands ($\lambda < 320$ nm) of the lamp emission spectrum. The cooling water flowing through the double-walled immersion well allowed us to eliminate the infrared spectrum of the light. The wavelength limit of the light for electron–hole creation is 387 nm because the bandgap of anatase is about 3.2 eV. Thus, the light spectrum of interest with a strong peak at the wavelength of 365 nm remained available for reaction. The suspension was stirred magnetically and the reactor was put in a water bath, which maintained the suspension temperature at $25 \pm 1\,^{\circ}C$ for a part of our experiments considering factors other than the effect of temperature. The lamp was preheated for 5 min before each experiment for obviating the poor irradiation of the lamp in the first several minutes. 500 ml/min of oxygen (Wright Brothers, 99.5%) was sparged into the solution from a gas distributor near the bottom of the reactor. The pH of the reaction suspension was not adjusted for experiments considering factors other than studying the effect of the pH. Samples of the reaction suspension were taken with a syringe at different time intervals and filtered with Cameo 25P polypropylene syringe filters (OSMONICS, Cat# DDP02T2550). The sample solutions were analyzed with a Total Organic Carbon Analyzer (TOC-VCSH, Shimadzu) and a pH electrode (Fisher, P.N. 13-620-112).

3. Results and discussion

The present study elucidates the effects of initial solution pH, initial concentration of DEPA, and temperature on kinetics of DEPA photocatalytic mineralization in aqueous suspension of the two types of TiO_2. These effects are reported and discussed in the order shown above. The results are based on measurements of complete mineralization of DEPA in terms of total organic carbon (TOC) concentration which represents the integral concentration of all organic compounds left in solution.

3.1. pH influence

Fig. 1 shows the TOC concentration curves during photocatalytic DEPA decomposition with HK and P25 at different initial pH values of the reaction mixture. All the curves follow the same λ-shaped pattern. During the first 20–60 min, TOC concentration decreases slowly, then follows a fast decrease, and finally the concentration reaches nearly zero. The photocatalytic decomposition of DEPA on TiO_2 goes through several consecutive steps that include oxidation of ethoxy groups, their elimination, and elimination and oxidation of aminogroup followed by oxidation. The main final products are CO_2, H_3PO_4, NH_3 and HNO_3, ammonia and nitrates being formed in variable ratio [15]. Thus, at the beginning of the oxidation partial oxidation products are formed and then they are mineralized.

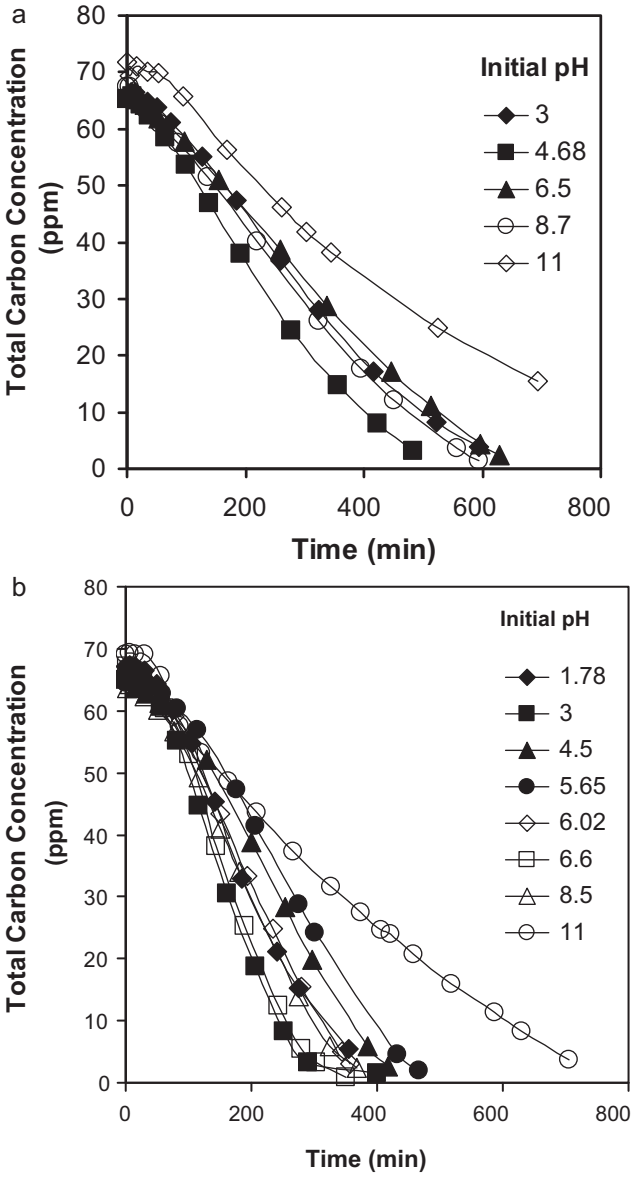

Fig. 1. Time course of the degradation of total carbon over (a) HK and (b) P25 at different initial pH. Catalyst concentration 0.25 g/l, initial DEPA concentration 200 mg/l, and reaction temperature $25 \pm 1\,^{\circ}C$.

The middle straight part of the kinetic curves was used for calculation of the mineralization rate. Fig. 2 shows the effect of pH on DEPA mineralization rate calculated as the slopes of the kinetic curves on the two photocatalysts used. There are several interesting features in this figure. The rate of mineralization on TiO_2 P25 is higher than that on TiO_2 HK at any pH. The rate forms maxima at two pH values different for different photocatalysts. For P25 the maxima are at pH 3 and 6.6, while for HK the maxima are less pronounced and located at pH 4.7 and 8.7. The reaction rates with both TiO_2 catalysts are the lowest at pH = 11.

The effect of pH on photocatalytic oxidation has been studied before for several substrates. The 4-chlorophenol oxidation rate on P25 is maximal at pH 7 and 12 while the mineralization rate decreases with increase in pH. For HK the oxidation rate is almost pH independent while the mineralization rate again decreases with an increase in pH. The concentration of intermediate products rises with increase in pH. The pH was kept constant during the reaction by a pH-stat [21]. With the same pH-stat technique, the rate of 1,2-diethyl phthalate oxidation and mineralization on TiO_2 HK was the

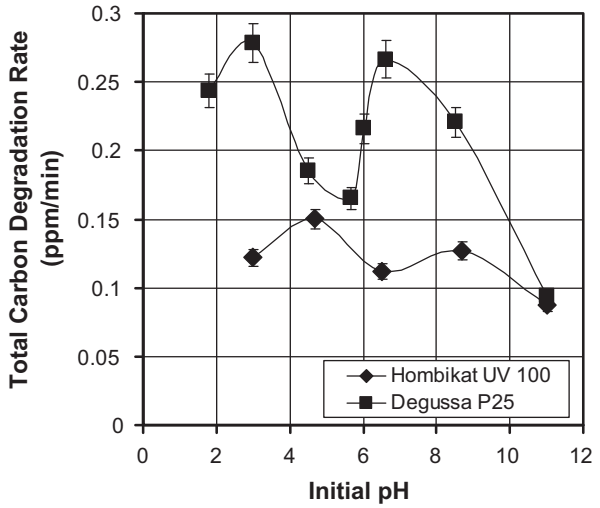

Fig. 2. Rate of total carbon mineralization on HK and P25 at different initial pH calculated from slopes of kinetic curves in Fig. 1.

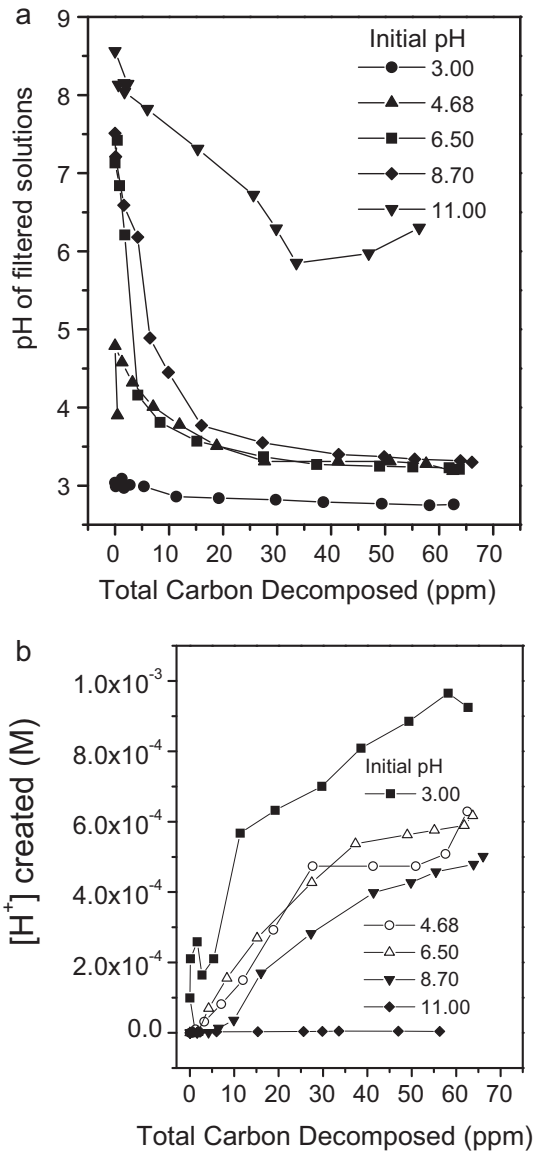

Fig. 3. pH of the filtered samples (a) and concentration of H^+ created (b) as a function of mineralized total carbon during the DEPA photodecomposition on Hombikat UV 100 at different initial pH values. TiO_2 catalyst concentration 0.25 g/l, initial DEPA concentration 200 mg/l, and reaction temperature 25 ± 1 °C.

highest at pH 6 [22] whereas it continuously increased with pH for chloroform [23]. The organophosphorous compound dimethyl methylphosphonate oxidation rate on TiO_2 P25 seems to be the highest for the initial pH 5.5. The pH decreased during the reaction and thus even the initial pH 10.5 resulted in the final pH of only 3.6 and the similar rate [24].

Amines show increased rate in basic media. The chlorethylammonium oxidation rate increased and become stable after pH reached 8 [23]. The 2-chloroaniline oxidation rate increases with an increase in pH on P25 up to the highest pH used of 9. The pH decreased during the reaction from 9 to about 5 [25]. The 2-(butylamino)ethanethiol mineralization rate was maximal at pH near 9 for both TiO_2 P25 and HK [26]. Oxidation did not proceed in acidic solution. The rate of oxidation of ammonia and methylene blue increased with pH and levels off at pH 9.5 [27] and 7 [28], respectively, whereas mineralization rate of methylene blue was maximal at pH 4 [29].

For azo dyes, the pH dependence can be different. Acid orange 7 which is an azo dye with sulfonic acid group demonstrated higher adsorption on TiO_2 P25 at pH 2 than at pH 6 and 12. However, the rate of discoloration was higher at pH 10–12 than at pH 2–9 [30]. Photocatalytic degradation rate of acid red 18 on ZnO increased monotonically with an increase of pH till the highest pH used 11 [31].

Oxidation of trichloroacetic acid became faster with decreasing pH through 1.5 [23]. The photodegradation rate on TiO_2 P25 of herbicide clopyralid which is a pyridine with the carboxylic acid group had two maxima at pH 3 and 9 [32].

From the reported experimental data it follows that electrostatic interactions play a key role in oxidation and mineralization. pH determines the charge of substrate and TiO_2. The pH of ZPC is 6.25 for Degussa P25 [33] and is higher for TiO_2 Hombikat UV 100. At pH below ZPC, the surface is charged positively and above ZPC it is charged negatively. The charge of the compound to be oxidized is determined by its pK_a and pH. Amines are protonated and positively charged at pH below p*K*a which is generally above 7. In acidic pH both the TiO_2 surface and the amine substrate are positively charged, repel each other and the reaction is retarded. For DEPA the p*K*a value is expected at ~8 [34]. Thus, the DEPA becomes mostly neutral at pH ~ 8 and above. The neutral molecule can be oxidized directly by valence band holes and attacked efficiently with OH• radicals. It is known that the protonated amines are not oxidized by holes and the rate constant with hydroxyl radical is much lower than with the neutral amines [34,35]. pH ~ 8 corresponds to the second maximum of the mineralization rate in Fig. 2.

Further oxidation of DEPA molecule produces diverse acids [15] which have pK_a below 7. As the literature reviewed above demonstrates, acidic substrates require for photocatalytic oxidation acidic pH close to pK_a. The acids forming in the photocatalytic oxidation decrease the pH of the reaction mixture as Fig. 3 demonstrates. If too high initial pH is taken the amount of acids produced in oxidation is not enough to decrease pH to the optimal value. This causes the rate of mineralization to decrease for initial pH above ~ 8.

The appearance of the first maximum of mineralization rate at pH ~ 4 (Fig. 2) cannot be explained by the above arguments because at pH < ~6 the DEPA molecule is protonated and, like other amines, not susceptible to photocatalytic oxidation. However, the DEPA molecule is known to undergo acidic hydrolysis with elimination of ethoxy groups [36]. The forming ethyl phosphoramidate (EPA) is acid with pK_{a1} ~ 3 that forms zwitterionic species in aqueous solutions [34]. If pH goes below pK_{a1}, the EPA molecule becomes positively charged and repels from the positively charged TiO_2 sur-

face. This causes the appearance of the first maximum of the rate dependence on pH at pH ~ 4. The exact position of the maximum depends on acid–base properties of TiO_2.

Fig. 2 shows the initial pH values of the reaction mixture. However, as it has been mentioned above, due to the formation of acids, pH decreases during the reaction. Fig. 3a shows the pH profiles and Fig. 3b reveals the additional concentration of protons created during photocatalytic oxidation of DEPA on TiO_2 HK. One can see that pH of the reaction mixture decreases and reaches nearly the same value ~3.5 for all starting pHs except 3 and 11. Thus, this pH seems to be optimal for oxidation of intermediate products and their mineralization. The intermediates of DEPA photocatalytic oxidation are acids such as diethyl phosphate, ethyl phosphate, acetic and hydroxyacetic acids, ethyl phosphoramidate, bis(2-hydroxyethyl) phosphate [15]. Appearance of these acids decreases pH and some increase of pH at the final stages of DEPA photocatalytic oxidation is attributable to conversion of organic acids such as acetic and hydroxyacetic into CO_2.

Fig. 3b shows that the concentration of protons created during the DEPA mineralization is different for the different initial pH. This can be partly due to the different ratio of the nitrogen-containing final products, ammonia and nitric acid, reported in [15] as about 2:1 and varying with reaction time. The main cause is considered to be the buffering effect of the TiO_2 surface which consumes different amount of protons for neutralization of basic hydroxyl groups for different initial pH.

Fig. 4a demonstrates the pH profiles for photocatalytic oxidation over TiO_2 P25. Again, the pH curves converge to steady pH near 3.5 except the starting pH values 11, 3, and 1.8. Therefore this pH is optimal for continuing the mineralization process. The optimal starting pH is higher. The concentration of protons created in DEPA mineralization over P25 has different profiles for the different initial pH (Fig. 4b). Only for the initial pH 1.8 can the final $\Delta[H^+]$ be considered approaching the theoretical value of ~2 mM according to the mineralization scheme shown below.

$$(C_2H_5O)_2P(O)NH_2 + 9O_2 \xrightarrow{TiO_2,\ h\nu} 4CO_2 + 4H_2O + H_3PO_4 + HNO_3.$$

3.2. Effect of DEPA concentration

Fig. 5a shows kinetic curves of DEPA mineralization over TiO_2 Hombikat UV 100 and Fig. 5b those for TiO_2 Degussa P25 at different initial concentration of DEPA. The rate of mineralization generally increases with the initial concentration. Fig. 6 demonstrates the relation of the DEPA concentration and the total carbon decomposition rate calculated from the slope of the linear part of kinetic curves in Fig. 5. One can see that for TiO_2 P25 the rate increases first with the DEPA concentration, reaches a maximum at the DEPA concentration of 200 mg/l (~1.3 mM), and then stays the same within experimental error with higher DEPA concentration. This observation is in agreement with the earlier observed maximum in the rate of dimethyl methylphosphonate oxidation [37], of trimethyl phosphate and thiethyl phosphate oxidation [38] on this photocatalyst at concentrations 1–2.5 mM. This phenomenon can be explained by the Langmuir–Hinshelwood mechanism with competition of DEPA and molecular oxygen for adsorption sites. Indeed, oxygen concentration in aqueous solutions is rather low (~0.25 mM) which makes competition of organic substrates with oxygen for adsorption sites efficient. For TiO_2 Hombikat the maximum is not observed and the rate increases with an increase in $[DEPA]_0$ monotonically. This can be related with different surface properties of TiO_2 Hombikat which offer surface sites for stronger oxygen adsorption.

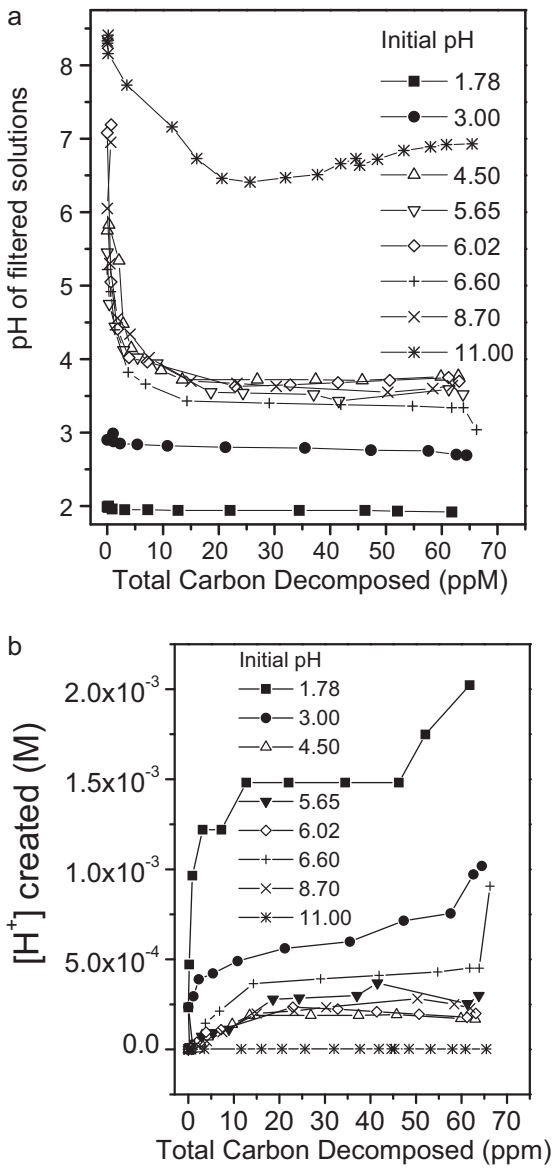

Fig. 4. pH of the filtered samples (a) and concentration of H^+ created (b) as a function of mineralized total carbon during the DEPA photodecomposition on TiO_2 Degussa P25 at different initial pH values. TiO_2 catalyst concentration 0.25 g/l, initial DEPA concentration 200 mg/l, and reaction temperature 25 ± 1 °C.

3.3. Effect of temperature

Fig. 7 shows the DEPA mineralization kinetic curves over HK (Fig. 7a) and P25 (Fig. 7b) taken at different reaction temperatures. It is observable that an increase in temperature resulted in faster mineralization of DEPA. Fig. 8 represents the Arrhenius plots for the mineralization rate calculated from the linear parts of the kinetic curves in Fig. 7. Two linear correlations are obtained if one plots the natural logarithm of the total carbon decomposition rate with respect to the reciprocal of temperature. The correlation results are summarized in Table 1. The activation energy for total carbon decomposition with HK and P25 is 29.5 ± 1.0 and 24.3 ± 3.1 kJ/mol,

Table 1
Correlation results of Fig. 8 according to the Arrhenius Equation $W = A \cdot e^{-E_a/RT}$.

	A, 10^3 mg/(l min)	E_a, kJ/mol
Hombikat UV 100	17 ± 6	29.5 ± 1.0
Degussa P25	7 ± 5	24.3 ± 3.1

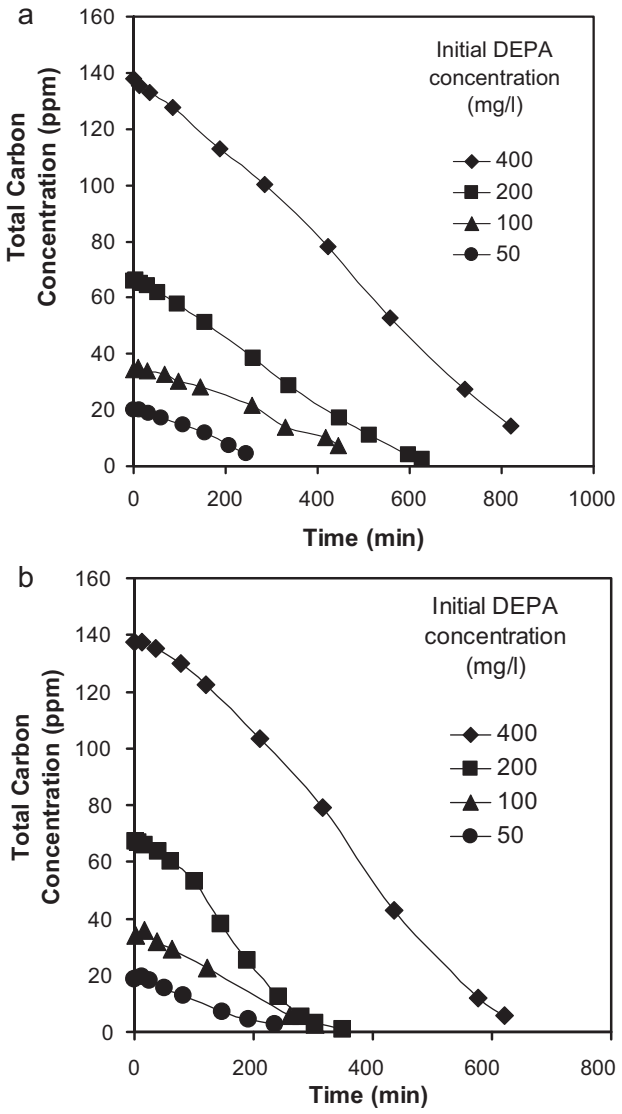

Fig. 5. Time course of the degradation of total carbon over (a) HK and (b) P25 starting from different initial DEPA concentrations. Catalyst concentration 0.25 g/l, reaction temperature 25 ± 1 °C, and pH was not adjusted.

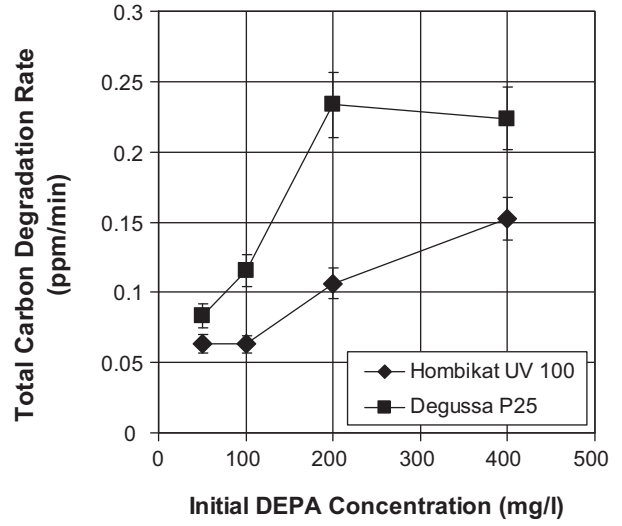

Fig. 6. Influence of the initial DEPA concentration on the total carbon mineralization rate over TiO_2 Hombikat UV 100 and Degussa P25. Catalyst concentration 0.25 g/l, reaction temperature 25 ± 1 °C, and pH was not adjusted.

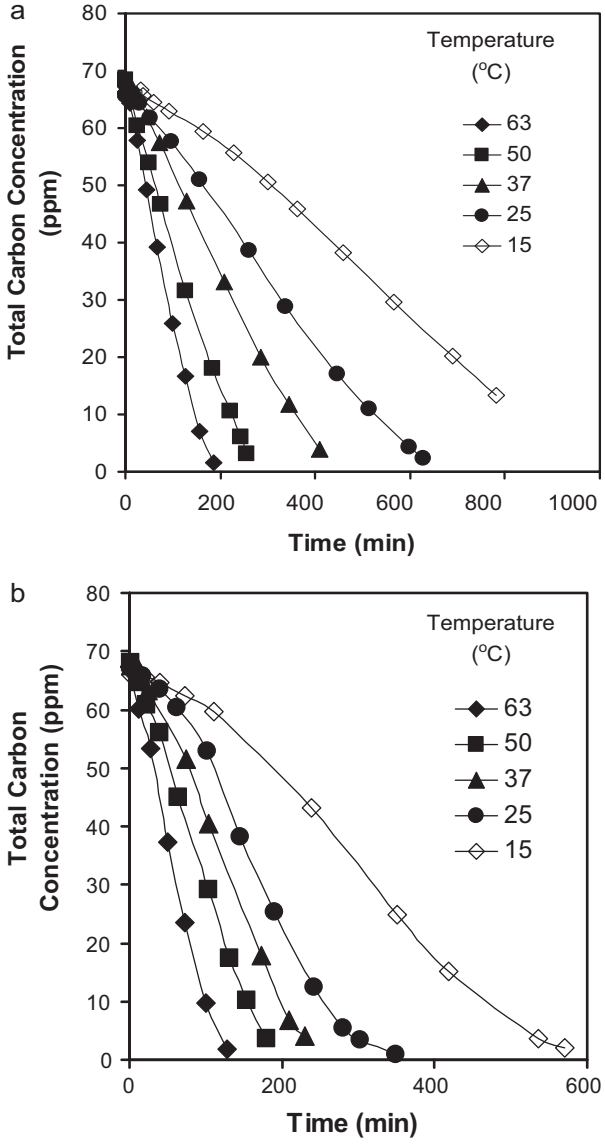

Fig. 7. Temporal profiles of the total carbon concentration during the DEPA oxidation on (a) HK and (b) P25 at different temperatures. Catalyst concentration 0.25 g/l, initial DEPA concentration 200 mg/l, and pH was not adjusted.

respectively. These activation energies are close to each other and fall within the previously reported values from 5.5 to 31 kJ/mol for photocatalytic oxidation of different organic compounds [29,32]. The DEPA mineralization activation energy is relatively large compared to the values reported in the literature and the difference is possibly due to the fact that, in contrast to disappearance rates of the starting compound reported in the literature, mineralization rate includes many consecutive stages of oxidation. Thus, the mineralization activation energy reflects the activation energy of the slowest reaction. Such a reaction can be a dark transformation of peroxyl radicals or tetroxides formed in the quick reactions with hydroxyl radicals and dissolved oxygen [15].

3.4. Effect of the TiO_2 concentration

Fig. 9 shows the dependences of the rate of total carbon mineralization on HK or P25 photocatalysts concentration during DEPA photodecomposition. The total carbon destruction rate with HK is increasing with the TiO_2 concentration increase. Two regions appear in the curve. When HK concentration is lower than 375 mg/l,

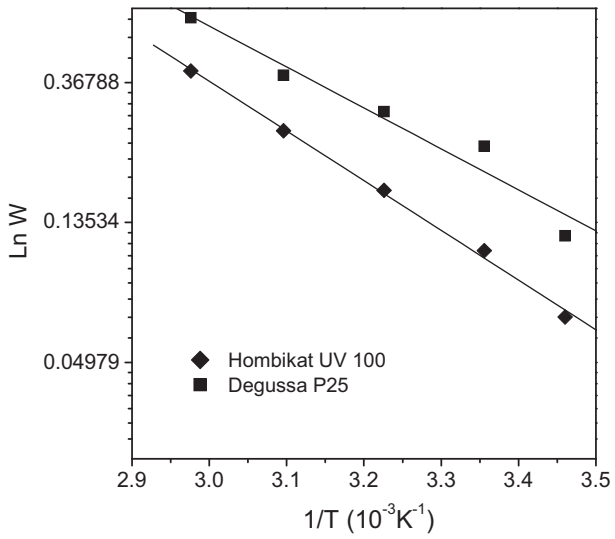

Fig. 8. Arrhenius plot for total carbon mineralization rate over TiO_2 Hombikat UV 100 and Degussa P25. Catalyst concentration 0.25 g/l, initial DEPA concentration 200 mg/l, and pH was not adjusted.

the rate increases about 0.026 ppm/min with every 100 mg/l HK concentration increase. When the catalyst concentration is higher, the rate increases only about 0.0023 ppm of carbon per min with every 100 mg/l HK concentration increase, which is one order lower than the number above. It indicates that with this critical HK concentration nearly all the light has been absorbed and utilized by TiO_2 for active oxygen species creation and DEPA destruction.

The curve shape of P25 is different. There is a peak appearing at the critical P25 TiO_2 concentration of 375 mg/l. The slope of the curve is 0.051 ppm carbon/min for every 100 mg/l P25 when P25 concentration is lower than the critical. The maximum in the dependence of organic compounds degradation rate on TiO_2 P25 concentration has been observed in other studies [22,26,32]. The reason for the decrease of the rate upon the addition of more P25 is the aggregation of TiO_2 particles, shorter light penetration path due to higher absorption coefficients of P25. Working illuminated volume [39] with P25 decreases faster than that with HK with the addition of TiO_2 catalyst.

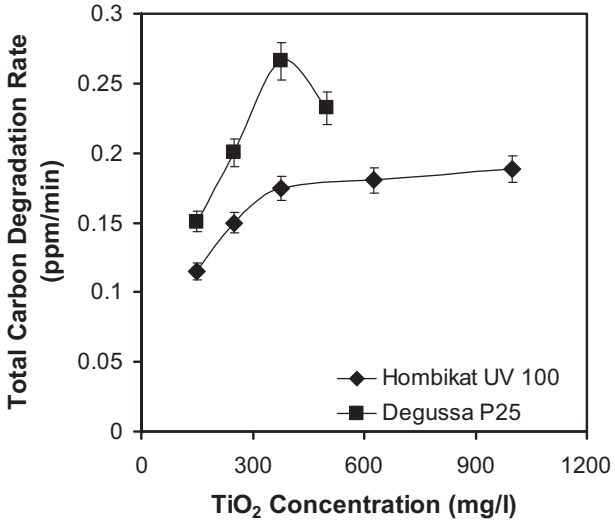

Fig. 9. The effect of photocatalyst concentration on the rate of total carbon mineralization on HK and P25. Initial pH 4.5 ± 0.2, initial DEPA concentration 200 mg/l, and reaction temperature 25 ± 1 °C.

4. Conclusions

Total oxidation of DEPA is observed with HK and P25 catalysts. We observed two ranges of pH where we achieved complete carbon decomposition, with one in the acid and one in near-neutral environments. The locations of these two peaks of P25 are different from those of HK. The highest rate was measured at optimal DEPA concentration at about 200 mg/l on P25 but the peak was not reached for HK. We found that the temperature dependence of the mineralization rate on P25 and HK obeys the Arrhenius equation. The activation energy for total carbon decomposition of DEPA over HK and P25 are 29.5 ± 1.0 and 24.3 ± 3.1 kJ/mol, respectively, with P25 being more efficient than HK. The decomposition rate over P25 increases faster than that over HK for each unit of TiO_2 added when TiO_2 concentration is less than 375 mg/l. The decrease of the reaction rate we observed above a certain concentration of P25 is due to its higher light absorption coefficient. In comparison, the reaction rate over HK increases slower with the concentration of the photocatalyst added.

Acknowledgements

The authors wish to acknowledge the NSF and the US Department of Army for partial support for this work through the grants CTS-0097347 and DAAD 19-00-1-0399, respectively. We also acknowledge funding from the Ohio Board of Regents (OBR) that provided matching funds for equipment to the NSF CTS-9619392 grant through the OBR Action Fund #333. President RF Grant for Leading Scientific Schools # NSh 3156.2010.3 is acknowledged.

References

[1] Y.C. Yang, J.A. Baker, J.R. Ward, Chem. Rev. 92 (1992) 1729.
[2] M.R. Hoffmann, S.T. Martin, W.Y. Choi, D.W. Bahnemann, Chem. Rev. 95 (1995) 69.
[3] D.F. Ollis, Environ. Sci. Technol. 19 (1985) 480.
[4] R.W. Matthews, Water Res. 20 (1986) 569.
[5] R.W. Matthews, J. Phys. Chem. 91 (1987) 3328.
[6] V. Augugliaro, L. Palmisano, A. Sclafani, Toxicol. Environ. Chem. 16 (1988) 89.
[7] C.S. Turchi, D.F. Ollis, J. Catal. 122 (1990) 178.
[8] D.F. Ollis, E. Pelizzetti, N. Serpone, Environ. Sci. Technol. 25 (1991) 1523.
[9] D.W. Bahnemann, Photochem. Convers. Stor. Sol. Energy (1991) 251.
[10] E. Pelizzetti, C. Minero, Electrochim. Acta 38 (1993) 47.
[11] G.W. Wagner, L.R. Procell, R.J. O'Connor, S. Munavalli, C.L. Carnes, P.N. Kapoor, K.J. Klabunde, J. Am. Chem. Soc. 123 (2001) 1634.
[12] G.W. Wagner, P.W. Bartram, O. Koper, K.J. Klabunde, J. Phys. Chem. B 103 (1999) 3225.
[13] G.W. Wagner, O.B. Koper, E. Lucas, S. Decker, K.J. Klabunde, J. Phys. Chem. B 104 (2000) 5118.
[14] A.V. Vorontsov, E.V. Savinov, L. Davydov, P.G. Smirniotis, Appl. Catal. B: Environ. 32 (2001) 11.
[15] A.V. Vorontsov, L. Davydov, E.P. Reddy, C. Lion, E.V. Savinov, P.G. Smirniotis, New J. Chem. 26 (2002) 732.
[16] Y.C. Chen, A.V. Vorontsov, P.G. Smirniotis, Photochem. Photobiol. Sci. 2 (2003) 694.
[17] T.N. Obee, S. Satayapal, J. Photochem. Photobiol. A: Chem. 118 (1998) 45.
[18] P.A. Kolinko, D.V. Kozlov, Environ. Sci. Technol. 42 (2008) 4350–4355.
[19] T. Hirakawa, N. Mera, T. Sano, N. Negishi, K. Takeuchi, Decontamination of chemical warfare agents by photocatalysis, Yakugaku Zasshi 129 (2009) 71–92.
[20] B. Sun, A.V. Vorontsov, P.G. Smirniotis, Langmuir 19 (2003) 3151.
[21] J. Theurich, M. Lindner, D.W. Bahnemann, Langmuir 12 (1996) 6368–6376.
[22] M. Muneer, J. Theurich, D. Bahnemann, J. Photochem. Photobiol. A: Chem. 143 (2001) 213–219.
[23] C. Kormann, D.W. Bahnemann, M.R. Hoffmann, Environ. Sci. Technol. 25 (1991) 494–500.
[24] K.E. O'Shea, S. Beightol, I. Garcia, M. Aguilar, D.V. Kalen, W.J. Cooper, J. Photochem. Photobiol. A: Chem. 107 (1997) 221–226.
[25] W. Chu, W.K. Choy, T.Y. So, J. Hazard. Mater. 141 (2007) 86–91.
[26] A.V. Vorontsov, Y.-C. Chen, P.G. Smirniotis, J. Hazard. Mater. B 113 (2004) 89–95.
[27] E.-M. Bonsen, S. Schroeter, H. Jacobs, J.A.C. Broekart, Chemosphere 35 (1997) 1431–1445.
[28] S. Lakshmi, R. Renganathan, S. Fujita, J. Photochem. Photobiol. A: Chem. 88 (1995) 163–167.
[29] T. Zhang, T. Oyama, A. Aoshima, H. Hidaka, J. Zhao, N. Serpone, J. Photochem. Photobiol. A: Chem. 140 (2001) 163–172.

[30] F. Kiriakidou, D.I. Kondarides, X.E. Verykios, Catal. Today 54 (1999) 119–130.
[31] N. Sobana, M. Swaminathan, Sep. Purif. Technol. 56 (2007) 101–107.
[32] D.V. Sojic, V.B. Anderluh, D.Z. Orcic, B.F. Abramovic, J. Hazard. Mater. 168 (2009) 94–101.
[33] C. Kormann, D.W. Bahnemann, M.R. Hoffman, Environ. Sci. Technol. 25 (1991) 494.
[34] S.J. Benkovic, E.J. Sampson, J. Am. Chem. Soc. 93 (1971) 4009–4016.
[35] G.V. Buxton, C.L. Greenstock, W.P. Helman, A.B. Ross, J. Phys. Chem. Ref. Data 17 (1988) 513–817.
[36] W.E. Steiner, B.H. Clowers, P.E. Haigh, H.H. Hill, Anal. Chem. 75 (2003) 6068–6076.
[37] E.A. Kozlova, A.V. Vorontsov, Appl. Catal. B: Environ. 77 (2007) 35–45.
[38] E.A. Kozlova, P.G. Smirniotis, A.V. Vorontsov, J. Photochem. Photobiol. A: Chem. 162 (2004) 503–511.
[39] J.F. Cornet, C.G. Dussap, G. Dubertret, Biotech. Bioeng. 40 (1992) 817.